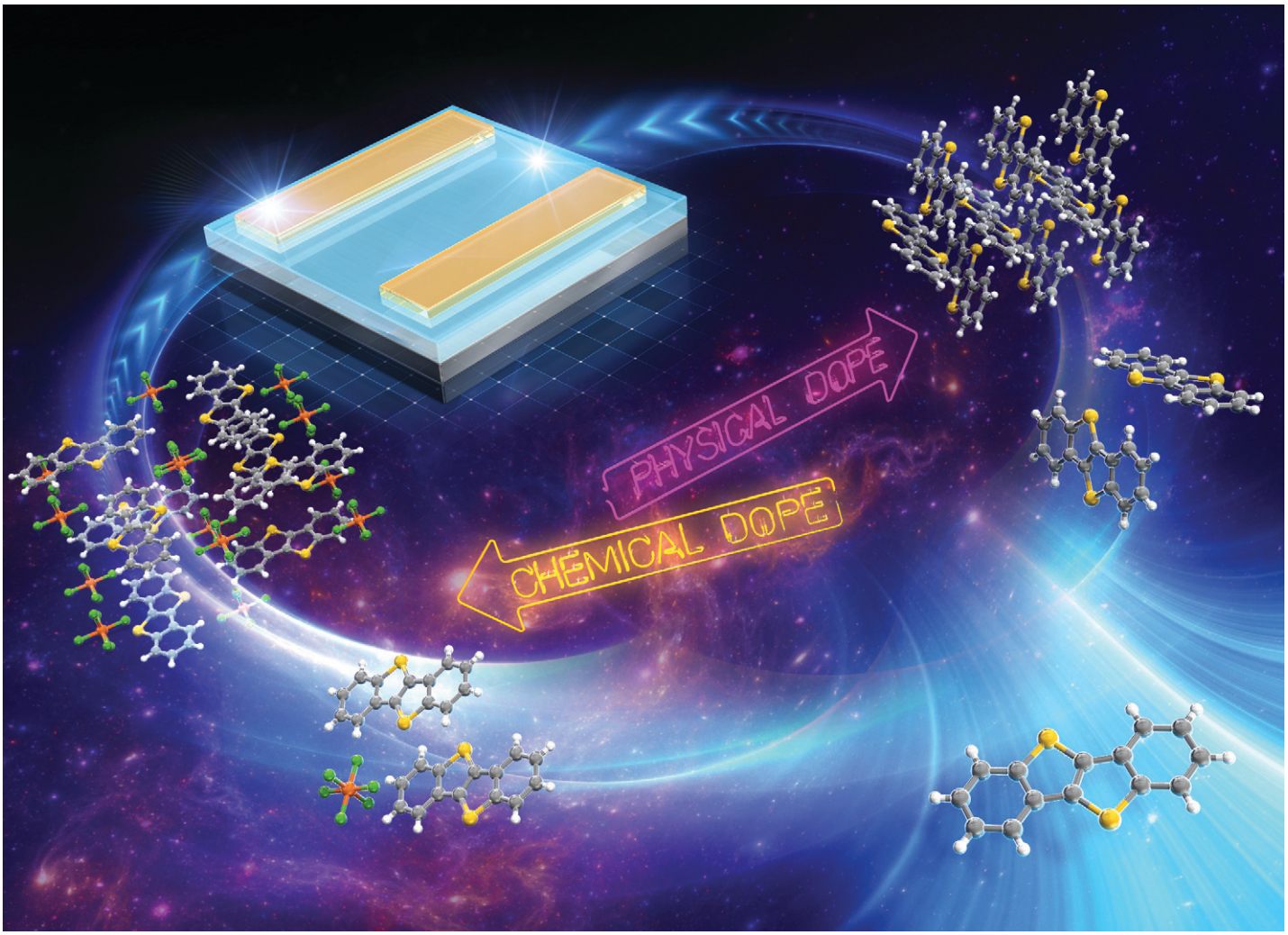

Showcasing research from Dr Tomofumi Kadoya, Department of Chemistry, Konan University, Kobe, Japan; and from Dr Toskiki Higashino, Research Institute for Advanced Electronics and Photonics, National Institute of Advanced Industrial Science and Technology (AIST), Tsukuba, Japan.

Boundary research between organic conductors and transistors: new trends for functional molecular crystals

This review highlights a unique transistor-fabrication method, so-called "self-contact" approach, in which the electrodes are formed from a part of the organic semiconductor thin film through chemical doping with dry and wet process, and will provide a valuable insight on the advantages and challenges for designing and developing next-generation organic electronic materials/devices.

As featured in:

See Tomofumi Kadoya *et al.*, *CrystEngComm*, 2023, **25**, 3846.

ROYAL SOCIETY OF CHEMISTRY

rsc.li/crystengcomm

Registered charity number: 207890

CrystEngComm

HIGHLIGHT

View Article Online
View Journal | View Issue

Cite this: *CrystEngComm*, 2023, **25**, 3846

Boundary research between organic conductors and transistors: new trends for functional molecular crystals

Tomofumi Kadoya *[a] and Toshiki Higashino *[b]

Received 30th March 2023,
Accepted 1st June 2023

DOI: 10.1039/d3ce00305a

rsc.li/crystengcomm

In organic transistors, the contact resistance at the interface between the organic semiconductor (OSC) and electrode reduces the device performance. To solve this problem, a buffer layer is inserted between the electrode and OSC layer to decrease the depletion layer that forms at the OSC surface. Especially in bottom-contact transistors, the effects of interfacial potentials and carrier traps can be suppressed using high-conductivity organic-conductors and carbon pastes as electrodes. Accordingly, a "self-contact" transistor was proposed based on chemically doping OSCs. This technique enables us to fabricate organic conductor electrodes specific to each OSC, resulting in transistors with low contact resistance. However, organic conductors based on OSCs are essential to expand the fabrication of these devices using the doping method. Consequently, OSCs have been used to develop a promising new class of organic conductors with high conductivity and excellent thermoelectric properties. Although developing organic conductors based on OSCs remains relatively unexplored, it is expected to become a new trend in functional molecular compounds.

1. Introduction

Organic semiconductors (OSCs) were ushered in by the discovery of electrical conduction in molecular crystals such as phthalocyanines and violanthrones in around 1950.[1,2] The room-temperature conductivity of these materials was approximately 10^{-10} S cm^{-1}, and such π-extended aromatic molecules were pointed out as intrinsic semiconductors.[3] The electrical conductivity of organic materials was greatly enhanced by the advent of charge-transfer (CT) complexes/salts (*e.g.* perylene–bromine salts showed a conductivity of 0.1–1 S cm^{-1}).[4] The partial CT state between the constituent electron donor and acceptor acts as a high-concentration chemical doping. This doping method is quite efficient and reliable for generating conduction carriers in molecular materials, and has led to a number of CT complexes/salts exhibiting metallic and even superconducting states, thus greatly expanding the field of organic conductors.[5–7] Needless to say, the progress in the field has been largely driven by the evolution of tetrathiafulvalene (TTF), a remarkably excellent donor.[8–12] Note that although these CT complexes/salts are, in many cases, formed as two- or multiple-component systems involving donors, acceptors, or inorganic ions, single-component organic conductors have also been developed through sophisticated molecular design and crystal engineering.[13–30]

Steady progress has been made with conventional OSCs over the years based on their design versatility, as well as their intriguing properties such as low-environmental-impact processability, cost-effective applications, inherent light weight, and flexibility. These OSCs features, in combination with physical methods for generating currents or voltages through photoexcitation, thermal gradients, and electric field effects, have led to the development of next-generation organic electronic devices such as organic photovoltaics (OPVs),[31–36] organic thermoelectrics (OTEs),[37–40] and organic field-effect transistors (OFETs).[41–47] Among them, OFETs provide a platform for investigating the intrinsic carrier transport properties of organic materials, as well as their application in switching devices. Typically, carrier injection into the organic active layer of OFETs produces semiconducting resistivity, but metallic states can also be achieved by tuning the carrier density using high-κ dielectrics such as ionic liquids.[48–52] Superconducting states can also be driven by controlling the band filling of Mott insulators.[53–55] In this case, field-effect carrier injection causes only the band filling of the active layer (target material) to change without any influence on the chemical composition. Therefore, this is a suitable method for the rapid and precise control of the

[a] *Department of Chemistry, Konan University, 8-9-1 Okamoto, Higashinada, Kobe 658-8501, Japan. E-mail: tkadoya@konan-u.ac.jp*
[b] *Research Institute for Advanced Electronics and Photonics, National Institute of Advanced Industrial Science and Technology (AIST), 1-1-1 Higashi, Tsukuba, Ibaraki 305-8565, Japan. E-mail: t-higashino@aist.go.jp*

carrier density near the Fermi level in strongly correlated electron systems.

The performance of OFETs has been limited by the contact resistance (carrier-injection barrier) at the semiconductor–metal interface.[56–59] OSCs do not generally form Ohmic junctions, in which the carrier-injection barrier is approximately zero, with metal electrodes, in contrast to inorganic semiconductors. This can be attributed to the degree of morphological disorder of OSC molecules and charge transfer at the metal–organic junctions, which create interfacial carrier traps and potential shifts.[43,46,60,61] In other words, the interface between the OSC and the metal electrode tends to be a Schottky junction where charge injection resistance exists. The details of Schottky junctions are complicated, for which various theoretical models have been proposed based on photoelectron spectroscopic (spectroscopy) evaluation.[61–64] Therefore, to improve device performance, various methods have been developed to minimize the contact resistance.

In this highlight, we first focus on the fundamental issue of contact resistance at the OSC–electrode interface in organic transistors, and introduce techniques to reduce the contact resistance, such as the insertion of buffer layers and use of CT-complex electrodes. Next, to fabricate CT-complex electrodes, we introduce a new type of OFET, which can be described as a "self-contact transistor", in which a part of the semiconductor is converted into a conducting material and directly used as an electrode. We then highlight recent studies on non-TTF-type organic conductors derived from high-performance OSCs.

2. Contact resistance at the organic semiconductor/metal electrode

2.1. Laminated buffer layers into semiconductor/electrode interfaces

The energy level between an OSC and an electrode is important when considering contact resistance. The simplest model is the Mott–Schottky model, which takes the difference between the work function E_W of the electrode and the highest occupied molecular orbital (HOMO) and lowest unoccupied molecular orbital (LUMO) levels of the OSC.[59,65] However, photoelectron spectroscopic experiments under ultrahigh vacuum have reported incorporating the value of the vacuum level shift into this Mott–Schottky model equation.[60–64,66] Nevertheless, deciding which model to apply can be challenging depending on the OSC/metal junction combination. In general, numerous carrier traps exist at the interface between the OSCs and metals. Therefore, even in the combination of OSCs and metal electrodes, which was originally expected to form an Ohmic junction, the carrier density becomes low owing to charge trapping, and the region behaves like a depletion layer. Such junctions often become Schottky junctions. At the Schottky interface, charge injection from the electrode to the semiconductor occurs *via* carrier migration through the depletion layer owing to the tunnelling effect. Therefore, increasing the carrier concentration at the electrode/semiconductor interface reduces the depletion layer thickness and enables effective tunnel injection.

As described above, the energy-level difference between the E_W of the electrode and the HOMO/LUMO levels of OSCs is a major factor in contact resistance. Thus, the OSC/electrode interface has been tuned by chemical modifications to align the energy levels. For example, some electron-donating/accepting materials are often used as n- or p-type dopants at the OSC/electrode interface. N-(p-) dopants must have a HOMO (LUMO) level shallower (deeper) than (or close to) the LUMO (HOMO) level of the matrix materials. The n-/p-dopants inject electrons/holes into the OSC surface. The resultant high charge density at the electrode/OSC interface improves the contact resistance by reducing of the width of the depletion layer and enhancing the tunnel injection.

As an example of OSC doping, Minari *et al.* demonstrated that contact p-doping using iron(III) chloride ($FeCl_3$) enables the improvement of the transistor characteristics of dioctylbenzothieno[3,2-*b*][1]benzothiophene (C8-BTBT) OFETs (Fig. 1).[67] Contact doping results in the formation of acceptor levels in the forbidden band and generates holes in the HOMO level edge of C8-BTBT. The induced holes significantly increase the charge density and passivate active traps at the contacts, significantly reducing the contact resistance from 200 to 8.8 kΩ cm. A strong organic acceptor, 2,3,5,6,-tetrafluoro-7,7,8,8-tetracyanoquinodimethane (F_4-TCNQ), also acts as a good p-type dopant. Abe *et al.* developed a method of controlling the threshold voltage of vacuum-deposited pentacene through F_4TCNQ doping while keeping a high field-effect mobility and on/off ratio.[68] Soeda *et al.* reported that the F_4TCNQ doping of solution-crystallised C8-BTBT produces high-mobility OFETs with a low threshold voltage and high on/off ratio in air.[69]

There are fewer n-type dopants than the p-type ones. Pyronin B chloride, TTF derivatives, 1,3-dimethyl-2-aryl-2,3-dihydro-1*H*-benzoimidazole (DMBI) derivatives, pentacene derivatives and organometallics have been reported as n-type dopants capable of electron injection.[70–75] In particular, the mechanism of DMBI dopants is complicated; a reaction between the dopant and host, which begins with either hydride or hydrogen atom transfer and ultimately leads to the formation of host radical anions is responsible for the n-doping effect.

Surface modifications of the source-drain electrodes are also effective for energy-level alignment. Self-assembled monolayers (SAMs) based on fluorinated molecules are used for bottom-contact devices with Au and Ag electrodes.[76–79] The E_W of the modified electrodes shifts more deeply to accurately match the HOMO level of p-channel OSCs, significantly improving the carrier injection and stability of the OTFTs. Not only do SAMs increase the carrier concentration, but they also reduce the disturbance of the thin-film morphology at the electrode–semiconductor

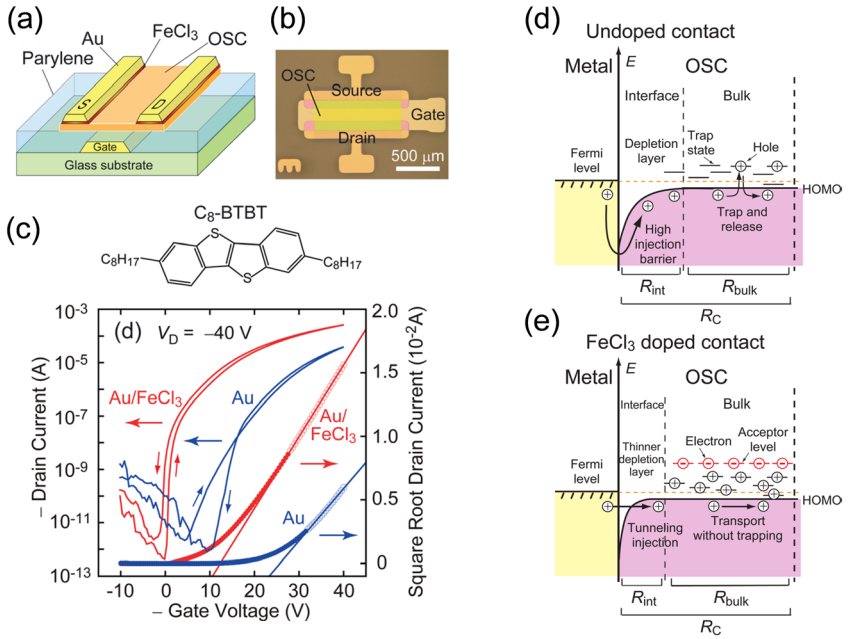

Fig. 1 (a) Schematic of OFETs based on C8-BTBT with a chemically doped contact. (b) Optical micrograph of an OFET device. (c) Molecular structure of C8-BTBT and typical transfer characteristics of the devices with doped and undoped contacts. The channel length and width of these devices are 100 and 1000 μm, respectively. (d) Energy diagram of the OSC device contact without acceptor doping. (e) Energy diagram of the OFET contact showing the reduction of Schottky barrier thickness and the occupation of trap states in the access region by charge carriers generated by acceptor doping at the contact. Reprinted with permission from ref. 67. Copyright 2012, AIP Publishing.

interface due to the lower surface energy. In the case of Ag and Cu electrodes, dimethyldicyanoquinonediimine (DMDCNQI) becomes a good candidate for electrode dopants, because it forms CT salts X(DMDCNQI)$_2$ (X = Cu and Ag), which act as a buffer layer.[80] The effect of the buffer layer can be interpreted as a reduction in the unfavourable interfacial potential for the charge injection between the semiconductor and the electrode. Note that the E_W of the Ag electrode shifts more deeply to approximately 5.3 eV by covering the electrode surface with a few nanometres of MoO_3 layer, leading to efficient hole injection into OSCs.[81]

2.2. Conducting organic materials as a low-contact-resistance electrodes

Contact resistance depends on the device structure of OFETs, as well as the energy level at the OSC/electrode junction. The electronic state at the junction differs between the bottom- and top-contact configurations, even in the same combination of OSCs and metals. This is closely related to the morphology of OSC molecules in the active layer. Generally, the morphology of OSC layers is strongly affected by the physically adsorbed substrate, to afford distinct molecular packing/orientation with those of the bulk crystal,

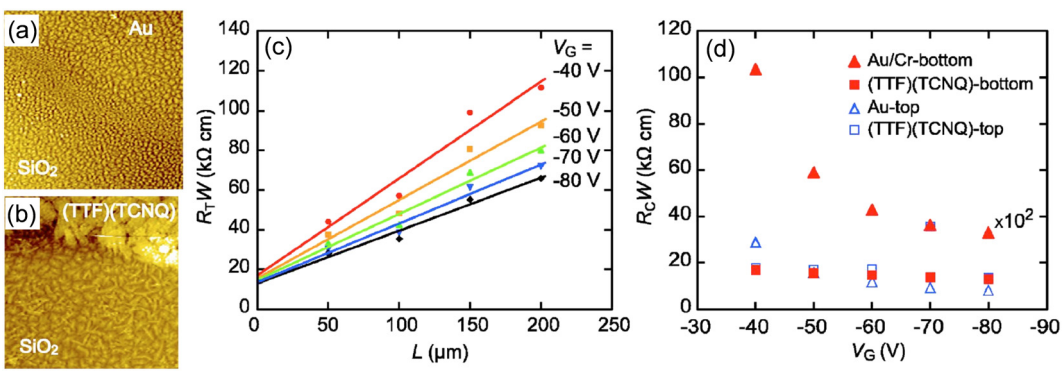

Fig. 2 AFM images of pentacene-based bottom-contact transistors, (a) near the channel electrode boundary for an Au-electrode transistor and (b) near the channel-electrode boundary for a (TTF)(TCNQ)-electrode transistor. (c) Analysis of contact resistance for bottom-contact (TTF)(TCNQ) transistors. (d) Gate voltage (V_G) dependence of the contact resistance R_cW. Contact resistance for bottom-contact Au transistors is multiplied by 1/100. Reprinted with permission from ref. 83. Copyright 2007, AIP Publishing.

which is known as thin-film phase. The morphological change largely depends on the surface energy of the substrate. Thus, it becomes more drastic when the OSC layer forms on the boundary region between the electrode and dielectric in bottom-contact OFETs, as seen in vacuum-deposited pentacene with the edge-on/face-on orientations. This morphological disorder causes a large contact resistance and significant degradation of the transistor performances (Fig. 2).[82,83] Thus, the contact resistance tends to be lower for top-contact devices, where the electrode is created later on top of the OSC layer. Even for bottom-contact devices, this morphological problem can be mitigated by treating the electrode surfaces with SAMs. However, a particularly simple and effective method is to use high-conductivity organic materials instead of metal electrodes. Because the surface energies of organic materials are almost the same with each other, the morphological change of OSCs are considerably suppressed.

For example, (TTF)(TCNQ), a well-studied CT complex,[84–87] can be used as an organic electrode, because of the high conductivity with metallic behaviour and the film-forming capability through vacuum deposition. When (TTF)(TCNQ) thin films are used as the electrode, the contact resistance is significantly reduced even with the bottom-contact device. The performance reaches nearly that of a top-contact Au-electrode device.[83] Moreover, the Fermi level of the CT complex can be controlled by changing the combination of the donor and the acceptor. Despite restrictions on the number of combinations, electron/hole injection into the OSC layer can be arbitrarily controlled.[88] Thus, organic electrodes not only eliminate the various factors that create depletion layers at the electrode-semiconductor interface, but also allow to control of the E_W of the electrodes. In addition to CT complexes, CT salts can become organic electrodes by utilizing the nanoparticles formed with ionic liquids or dispersant polymers, instead of the vacuum deposition method.[89,90] The nanoparticles are prepared as inks that disperse homogeneously in polar solvents, such as ethanol and water, enabling the use of simple solution processes to form conductive organic films. Alternatively, conductive carbon paste can be adapted to similar low-contact-resistance electrodes using a solution method (Fig. 3(a)).[91–93] Carbon paste is also attractive because it is less expensive than metal paste. High-resolution carbon electrodes can be created from carbon paste by laser sintering. This technique provides a short-channel transistor with a channel length of approximately 2.5 μm, without using photolithography. The resulting carbon films are as thin as 60 nm and has high transparency, it is a promising candidate for an electrode material to replace indium tin oxide.

2.3. "Self-contact" transistors using chemically doped organic-conductor electrodes

Many OSCs, regardless of their carrier type, undergo carbonization through heat treatment by laser irradiation.[94,95] The carbonized part in the OSC layer has sufficient conductivity for using as transistor electrodes (Fig. 3(b)). Such simple method for creating carbon electrodes by laser irradiation is applicable for various OSCs such as pentacene, oligothiophene, phthalocyanine, and C_{60}.[96] This type of transistor is called a "self-contact organic transistor" because the electrode is created directly from the OSC itself (Fig. 3(c)). Unfortunately, the carbon electrode in the self-contact transistors shows a relatively large contact resistance comparable to that of the bottom-contact Au-

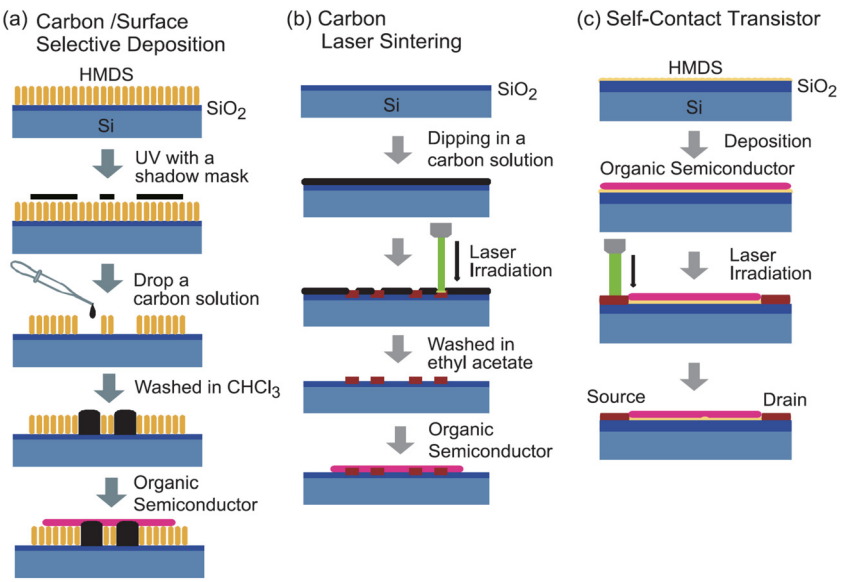

Fig. 3 Schematics of (a) solution-processed carbon electrodes, (b) laser-sintered short channel carbon electrodes, and (c) laser-irradiated self-contact transistors. Reprinted with permission from ref. 93. Copyright 2011, The Chemical Society of Japan.

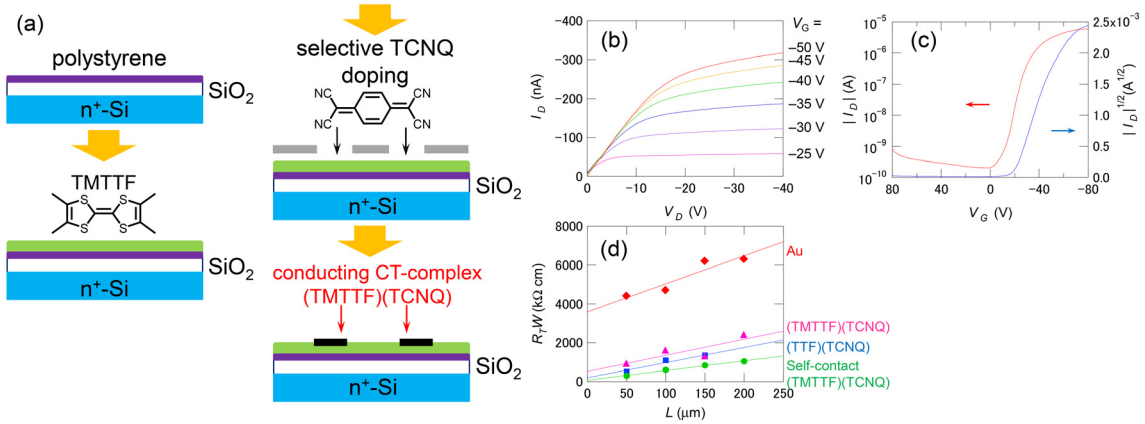

Fig. 4 (a) Schematics of the fabrication procedure of the chemical-doped self-contact transistors. (b) Output and (c) transfer characteristics of a self-contact transistor based on TMTTF/(TMTTF)(TCNQ). (d) Channel length dependence of the total resistance R_T normalized with respect to the channel width W for the top-contact transistors. Reprinted with permission from ref. 97. Copyright 2013, AIP Publishing.

electrode device, because of the morphological mismatch at the electrode–OSC boundary caused by the laser irradiation. However, the unique concept provides an opportunity to reduce the contact resistance using organic electrodes of CT complexes/salts directly formed by the OSC layer. Since most OSCs are either electron donors or acceptors, they can form highly conducting CT complexes/salts such as (TTF)(TCNQ) with appropriate chemical doping. Thus, the OSC layer can be selectively converted into organic electrodes to form chemical-doped self-contact transistors.[97–99] Fig. 4 shows an example of a combination of a tetramethyl-TTF (TMTTF) semiconductor and a (TMTTF)(TCNQ) electrode. The TMTTF film on a polystyrene-coated substrate is selectively converted into (TMTTF)(TCNQ) by the vacuum deposition of TCNQ through a metal mask and the subsequent thermal annealing. The resulting self-contact transistors exhibit low contact resistance and good carrier-transport characteristics, similar to standard top-contact Au-electrode devices. In addition to vacuum evaporation, inkjet printing has been applied for doping. The inkjet method allows to use organic electrodes derived from CT salts, which are usually decomposed *via* vacuum evaporation. Conductive $Cu(DMDCNQI)_2$ electrodes have been fabricated *via* inkjet printing of a CuI solution on a DMDCNQI semiconductor surface. The resulting transistors show stable n-channel operation and nearly the same performance as those of top-contact Au-electrode devices.[99] Furthermore, this doping method has been used to successfully fabricate flexible self-contact transistors composed entirely of organic materials, including electrodes.[98]

After chemical doping, the CT complex has a partially filled energy band. In the case of $Cu(DMDCNQI)_2$, the CT complex is an anion-radical salt and this ensures that the electron transport is maintained by the organic acceptor. In $Cu(DMDCNQI)_2$, Cu is $Cu^{4/3+}$ and DMDCNQI has a −2/3e charge. Therefore, the resulting LUMO band derived from DMDCNQI is 1/3 filled. When the center of the $Cu(DMDCNQI)_2$ band is located at the same position as the original LUMO level of DMDCNQI (4.65 eV), after the band formation with a bandwidth of 0.8 eV and electrons are only 1/3 filled in the entire band, the Fermi level is shifted down by approximately 0.1 eV from the original LUMO level

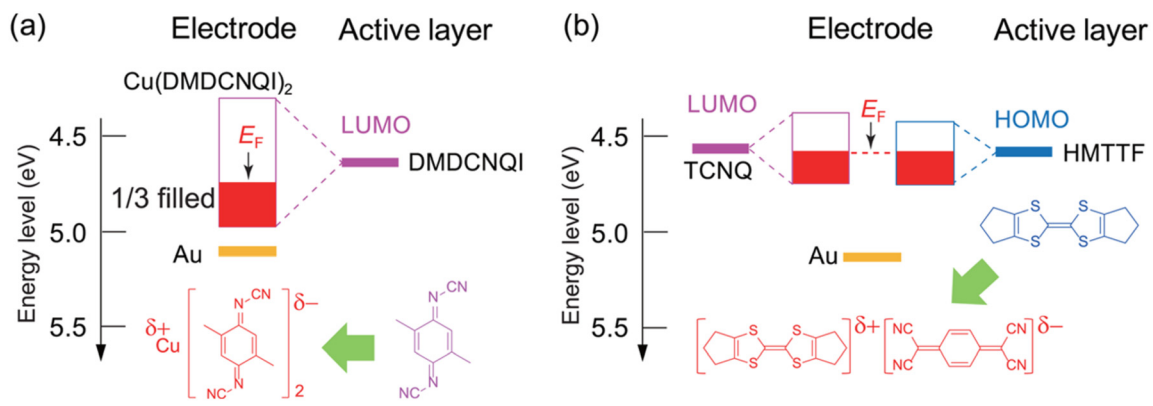

Fig. 5 Energy-level alignment between the semiconductors and electrodes in self-contact (a) DMDCNQI/$Cu(DMDCNQI)_2$ and (b) HMTTF/(HMTTF)(TCNQ) transistors. Reprinted with permission from ref. 88. Copyright 2014, American Chemical Society.

(Fig. 5a). On the other hand, the DA complex forms energy bands from both the donor and acceptor molecules. Upon band formation from both the donor and acceptor molecules, the Fermi level is expected to be located in between the HOMO of the donor and LUMO of the acceptor. Consequently, the Fermi level is located close to the energy level of the semiconductor layer (Fig. 5b).

The reported self-contact transistors have used redox-active materials such as TTF derivatives and DMDCNQI, which are well-known from studies on organic conductors. However, conventional OSCs of aromatic hydrocarbons such as pentacene and C_{60} hardly form atmospherically stable and highly conducting organic conductors. Thus, doping techniques have not been widely used in OFETs, in contrast to inorganic silicon, in which chemical doping has become standard. In the case of OSCs that do not form stable CT complexes, the conductivity in the doped electrode area is temporarily improved, but diffusion of dopants occurs, resulting in a decrease in the conductivity of the electrode. CT complexes that are stable as solids or crystals with strong intermolecular forces are necessary for self-contact transistors. Therefore, highly conductive organic conductors with excellent OSCs must be developed to expand the application of the chemical-doped devise fabrication.

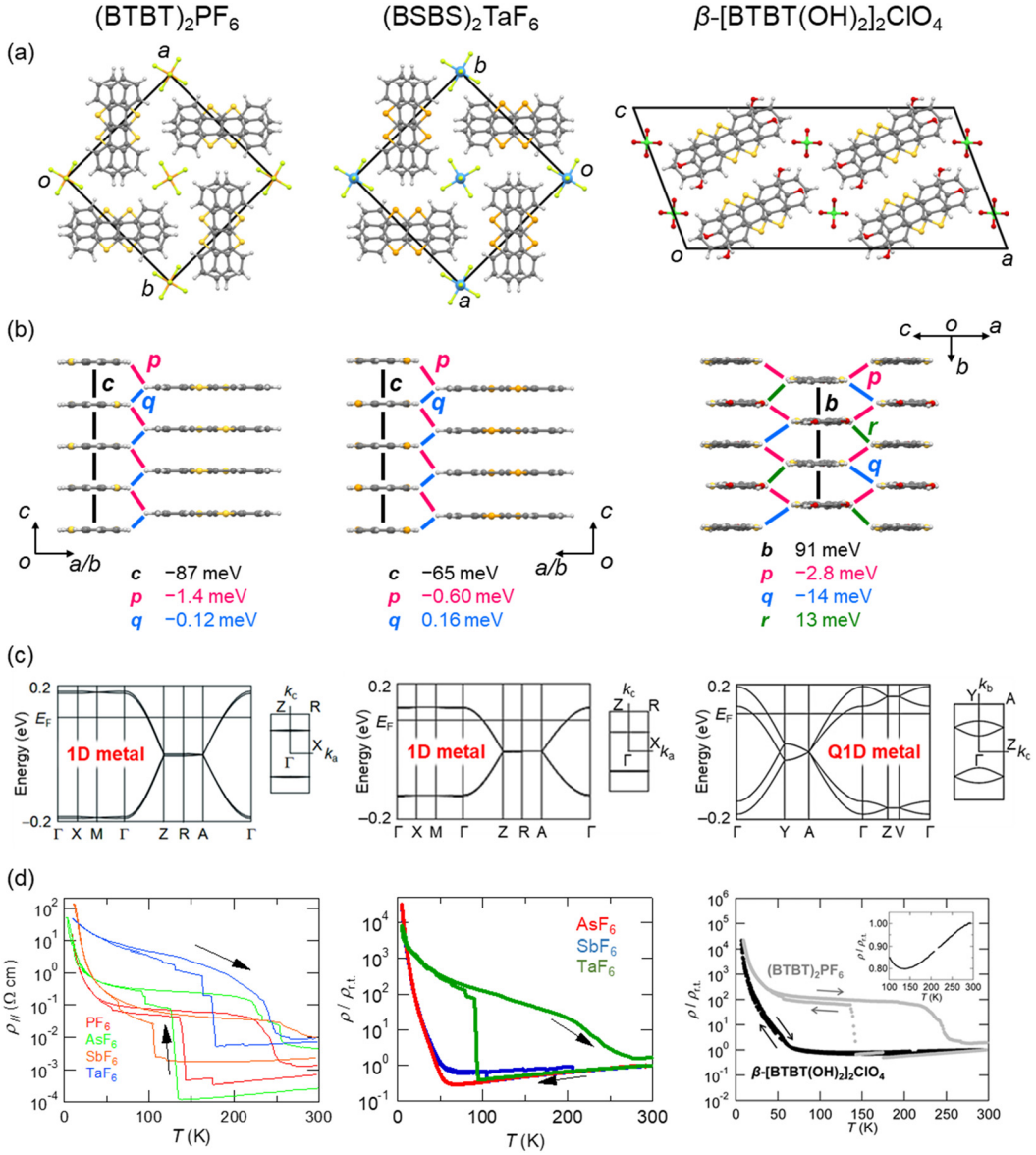

Fig. 6 (a and b) Crystal structures of $(BTBT)_2PF_6$ (CSD ref code: AFEBIY),[165] $(BSBS)_2TaF_6$ (CSD ref. code: ZOJREX),[167] and β-$[BTBT(OH)_2]_2ClO_4$ (CSD ref code: XAMRUB),[174] respectively. Transfer integrals between the BTBT (BSBS) molecules are shown. Anions are omitted for clarity. (c) Band structures and (d) electrical resistivities of BTBT salts (left, reprinted with permission from ref. 166. Copyright 2016, American Chemical Society), BSBS salts (middle, reprinted with permission from ref. 168. Copyright 2019, American Chemical Society), and $BTBT(OH)_2$ salts (right, reprinted with permission from ref. 174. Copyright 2017, Royal Society of Chemistry), respectively.

3. Organic conductors based on organic semiconductors

The essence of self-contact transistors is that both the active layer and the electrode are comprised from the same OSC materials to reduce the energy level and morphological mismatch at the interface, thereby significantly suppressing the contact resistance. Thus, an important requirement for high-performance self-contact transistors is that OSCs possess both excellent inherent transistor properties and abilities to form highly conducting CT complexes/salts. In this regard, TTF derivatives may become ideal candidates because they can mostly exhibit p-channel behaviour with high mobility and can easily form highly conducting CT complexes/salts.[42,90,100–102] However, such TTF-based OSCs are usually difficult to maintain long-term air stability due to their low ionisation potential of about 4.8 eV.[103–106] Meanwhile, highly conducting CT complexes/salts have been reported even for non-TTF-type donors, such as perylene[107–112] and fluoranthene,[113–116] dithiapyrene,[117–123] and chalcogen-bridged acenes,[124–136] but the transistor properties of these donors are still limited.[137–144] This section describes a new class of non-TTF-based organic conductors derived from high-performance OSC materials.

3.1. BTBT-based CT salts

Benzothieno[3,2-*b*][1]benzothiophene (BTBT) is a promising π-electron skeleton for high-performance p-channel OSCs that exhibits high intrinsic mobility and chemical stability.[145–163] The excellent hole transport capability of the BTBT materials is attributed to their two-dimensional (2D) crystal/electronic structures including short intermolecular contacts between the sulphur atoms with large HOMO coefficients. The high stability of the BTBT derivatives is associated with the deep HOMO level (E_{HOMO}), *ca.* 5.65 eV for the unsubstituted BTBT. This contrasts pentacene (E_{HOMO} = 4.85 eV)[164] and TTF derivatives (E_{HOMO} = 4.8 eV). Despite the weak electron-donating ability, BTBT can form CT salts with anions by electrochemical oxidation.[165] The first reported BTBT-based CT salt is $(BTBT)_2PF_6$, which comprises one PF_6 anion for every two BTBT molecules (Fig. 6). Thus, the BTBT molecule is partially oxidised with a +0.5e charge, and the salt forms a typical 3/4-filled band structure. In the crystal, the BTBT molecules form π-stacking 1D columns arranged in a windmill manner, in contrast to a herringbone packing seen in most neutral BTBT derivatives. These unique 1D columns are maintained even when PF_6 is replaced by other octahedral anions, such as AsF_6, SbF_6, and TaF_6.[166] All of these salts exhibit metallic behaviour. In particular, the AsF_6 salt exhibits the highest conductivity of 4100 S cm^{-1}, corresponding to a drift mobility of 16 cm^2 V^{-1} s^{-1}. This value is prominently high among the non-TTF-based organic conductors. The high conductivity is attributed to an extremely large transfer integral of approximately 350 meV between the π-stacking BTBT molecules, as revealed by the thermoelectric power and reflection spectra analyses. All these salts undergo a discontinuous resistivity jump during the cooling process, which can be suppressed by physical hydrostatic pressure on the crystal and chemical modifications of the BTBT molecule as described below. Further cooling makes these salts insulating due to the 1D instability. Magnetic susceptibility and spectroscopic experiments suggest that the insulating state is attributed to a $4k_F$ charge-density wave with a slight dimerisation of BTBT molecules.

Benzoseleno[3,2-*b*][1]benzoselenophene (BSBS) is a selenium analogue of BTBT, and forms CT salts $(BSBS)_2X$ (X = AsF_6, SbF_6 and TaF_6; Fig. 6), which are isostructural to the BTBT salts.[167,168] Such heavy chalcogen substitutions have been frequently used in TTF-based organic conductors to enhance the intermolecular interactions, leading to a significant increase of the electrical conductivity and a complete suppression of the metal–insulator transition.[169–173] This chemical modification to stabilise the metallic state is also effective in the BTBT system. The discontinuous resistivity jumps seen in the BTBT salts are shifted to lower temperatures or completely suppressed in the BSBS salts. However, the room-temperature conductivities are slightly less than those of the BTBT salts. The metallic state can also be stabilised by controlling the molecular arrangement using hydrogen-bonding interactions. Dihydroxy-substituted BTBT ($BTBT(OH)_2$) involves a catechol substructure with a strong hydrogen-bonding ability, producing a CT salt with a tetrahedral ClO_4 anion (Fig. 6), where the donor : anion stoichiometry is 2 : 1.[174] The resulting salt, $[BTBT(OH)_2]_2ClO_4$, forms hydrogen-bond chains through the catechol moiety of $BTBT(OH)_2$ and the ClO_4 anion, consequently constructing a sheet-type (so-called β-type) molecular arrangement of $BTBT(OH)_2$. This 2D molecular packing increases the dimensionality of the electronic structure from 1D to quasi-1D (Q1D) and consequently stabilises the metallic state, which is reminiscent of the very early days of TTF-based superconductors.[161,162] Note that this molecule shows a quinoid-like bond alternation upon oxidation especially in the central thienothiophene part, as is well-known in oligothiophenes.[175–178] These studies demonstrate that functionalised BTBT derivatives are promising electron donors in molecular conductors.

3.2. BTBT-based CT complexes

BTBT molecules form CT complexes when combined with strong organic acceptors. The first report on BTBT-based complexes is in combinations of alkylated BTBT (C_n-BTBT: n = 10) and TCNQ derivatives with a 1 : 1 composition. The BTBT and TCNQ molecules form an alternating mixed-stack structure.[179] Therefore, these complexes do not exhibit metallic conductivity, in contrast to the segregated-stack complexes represented by (TTF)(TCNQ) and the above-mentioned BTBT-based salts. The mixed-stack complexes form a unique layered crystal structure in which the

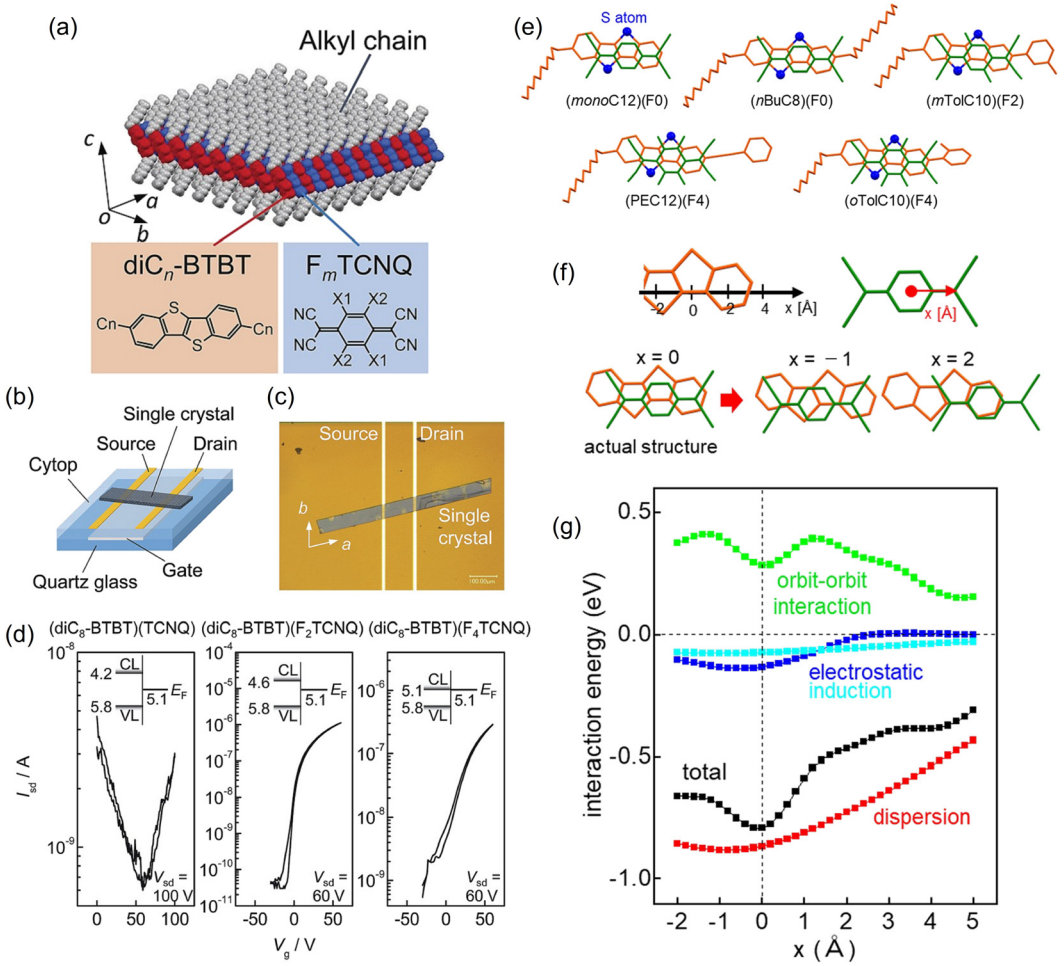

Fig. 7 (a) Molecular and crystal structures of (diC$_n$-BTBT)(F$_m$TCNQ) (n = 4, 8, and 12, m = 0, 2, and 4). (b) Schematic and (c) photograph of a single-crystalline OFET fabricated from (diC$_8$-BTBT)(F$_m$TCNQ). (d) Transfer characteristics of (diC$_8$-BTBT)(F$_m$TCNQ). Inset shows the interfacial energy-level alignment between (diC$_8$-BTBT)(F$_m$TCNQ) and the gold source/drain electrode. CL and VL are the conduction and valence levels of (diC$_8$-BTBT)(F$_m$TCNQ), respectively. E_F is the Fermi level of the Au source/drain electrode. Reprinted with permission from ref. 180. Copyright 2015, Royal Society of Chemistry. (e) Intermolecular arrangements of five TCNQ complexes BTBT derivatives along the alternating stacking axis. Sulphur atoms are represented by blue-filled circles. (f) Coordinates of BTBT and TCNQ core skeletons for the calculation of the intermolecular interaction energy with a fixed intermolecular distance. Origin of the x axis is set at the actual structure. (g) Profiles of total interaction and respective contributions by dispersion, electrostatic, induction, and short-range orbit-orbit interaction. Reprinted with permission from ref. 199. Copyright 2022, Royal Society of Chemistry.

π-conjugated moieties of the BTBT skeleton and TCNQ molecules are arranged in alternating 2D packing, regardless of the number of the fluorine atoms in F$_m$TCNQ (m = 0, 1, 2, and 4) and the alkyl-chain length of the C$_n$-BTBT (n = 4, 8, and 12; Fig. 7).[180] These TCNQ complexes of alkylated BTBTs exhibit basically n-channel semiconducting properties when used as an OFET active layer, as demonstrated in single crystals obtained by recrystallisation, polycrystalline thin films fabricated by vacuum deposition,[181] and unidirectional crystalline films prepared by solution coating.[182] The electron transport has long-term stability in air, which is ascribed to the sufficiently deep conduction levels of these complexes.[183] The dominance of electron transport is explained by the super-exchange mechanism closely related to the orbital symmetry matching, where transfers corresponding to the acceptor-to-acceptor hopping are considerably larger than the donor-to-donor hopping.[184–188] Interestingly, these complexes can also be formed by molecular thermal diffusion in bilayers consisting of single-component films[189] The pristine bilayers with F$_4$TCNQ stacked on C$_{10}$-BTBT show p-channel operation as well as single-component C$_{10}$-BTBT films. In contrast, thermal annealing of the stacked films promotes only n-channel transport, indicating that the CT complexes are formed in the whole film. This carrier polarity conversion can be controlled by adjusting the molar ratio of C$_{10}$-BTBT and F$_4$TCNQ in the stacked film.

The unsubstituted BTBT and BSBS can form mixed-stack CT complexes with (fluorinated) TCNQs and a π-extended analogue, tetracyanonaphthoquinodimethane (TNAP).[190–196] These complexes have charge transfer degrees of

approximately 0.1, irrespective of the acceptor strength, as revealed by the bond length analysis of the acceptor, the CN stretching frequency shifts, and the Raman spectra shifts. Thus, these complexes are classified as neutral complexes. The charge transfer degrees increase in the range of about 0.2 to 0.3 using alkoxy-substituted BTBT derivatives which are slightly stronger donors.[197,198] Regardless of the type of BTBT donors, these TCNQ complexes exhibit robust electron transport with excellent ambient and long-term stability. Recently, it has been found that most of the co-crystals of BTBTs and TCNQs have common intermolecular stacking arrangements between the planar donor and acceptor skeletons, irrespective of the type of substituent (Fig. 7).[199] The dispersion force is the primary force of attraction between the donor and acceptor and the repulsive short-range (orbit–orbit) interactions play important roles in determining the stacking configuration in the co-crystals. However, it was often claimed that CT interactions could be the main contributors to the attraction in donor–acceptor compounds.

3.3. Extension of dimensionality in non-TTF-type conductors

Solid-state physics in low-dimensional electronic systems has progressed from 1D conductors as typified by (TTF)(TCNQ), and the dimensionality of the electronic structures in organic conductors has been extended by elegant molecular designs. Bis(ethylenedithio)tetrathiafulvalene (BEDT-TTF) is a pioneer TTF to form CT complexes with a rich variety of 2D molecular arrangements depending on the combined anions.[200–214] This is attributed to the ethylenedithio group (*i.e.*, 1,4-dithiin ring) on the outside of the BEDT-TTF molecule, which plays two important roles:[215–219] 1) the sulphur atoms increase the overlap of molecular orbitals in the molecular-short direction. 2) The carbon atoms suppress simple π-stacking by protruding sterically above and below the TTF plane. Such molecular designs have provided a large number of CT salts composed of BEDT-TTF and its analogues in various orientations,[5,46,220,221] which have exhibited exotic physical properties such as superconducting transitions above 10 K,[222–227] non-equilibrium charge ordering,[228–232] metal–Mott insulator transitions,[233–238] a zero-band-gap state,[239–244] and quantum spin liquids,[245–252] further advancing the materials science in organic conductors.

Recently, a non-TTF-type 2D CT salt, (BEDT-BDT)PF_6 (BEDT-BDT = benzo[1,2-*g*:4,5-*g*]bis(thieno[2,3-*b*][1,4]dithiin)), has been reported (Fig. 8).[253] In this salt, the donor comprises a thienoacene π-core like BTBT and ethylenedithio groups similar to BEDT-TTF. This report has demonstrated that introducing substituents with high structural degrees of freedom, such as ethylenedithio groups, is quite effective in extending the dimensionality of non-TTF-type conductors as well as TTF systems. In contrast, the conventional non-TTF-type conductors mostly have a 1D crystal/electronic structure (as seen in perylene, fluoranthene, phthalocyanine, chalcogen-bridged acene, and dithiapyrene systems). The

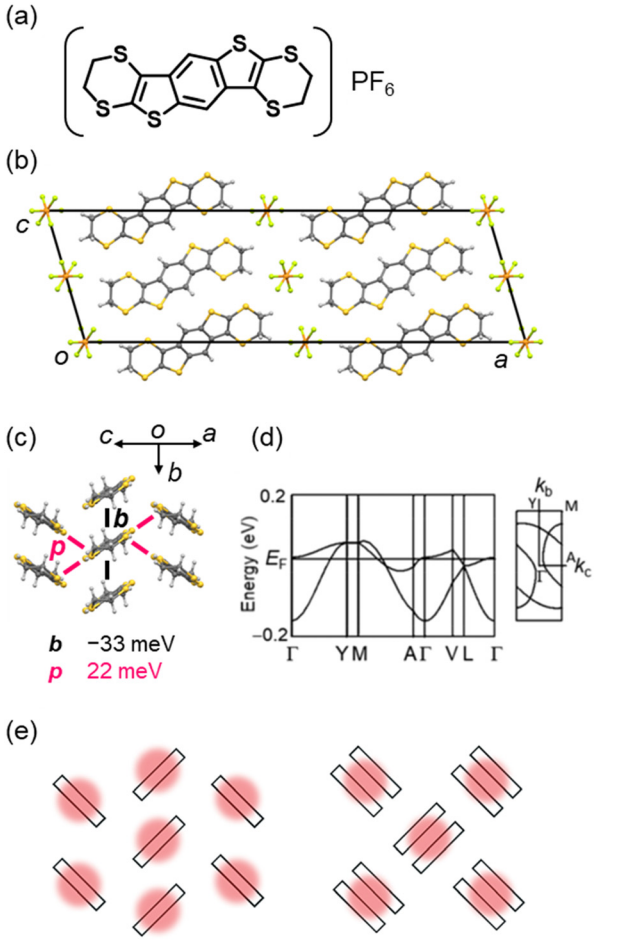

Fig. 8 (a) Chemical structure of (BEDT-BDT)PF_6. Crystal structures of θ-(BEDT-BDT)PF_6 (CSD ref code: FUSFEH),[253] viewed along (b) the π-stacking (crystallographic *b*) direction and (c) the molecular long-axis direction with the intermolecular transfer integrals (PF_6 anions are omitted for clarity). (d) Electronic band structures of θ-(BEDT-BDT)PF_6. (e) Schematics of the hole distribution in a genuine Mott insulator with a θ-type molecular packing (left) and a representative dimerized Mott insulator with a κ-type molecular packing (right). Reprinted with permission from ref. 253. Copyright 2020, Royal Society of Chemistry.

BEDT-BDT salt is formed by a 2D donor arrangement classified as a θ-type (herringbone-like) packing in a 1:1 composition with an octahedral anion PF_6. This contrasts to the neutral BEDT-BDT crystal,[254] which forms a pitched π-stacking similar to that of rubrene, one of the most high-performance OSCs.[255–258] The salt is a genuine Mott insulator with a hole localised in a molecule without any dimerisation in contrast to representative Mott insulators based on BEDT-TTF with a κ-type dimerised molecular packing,[259] and exhibits semiconducting behaviour because of the strong electronic correlations. The 2D electronic structure of the salt has been confirmed by tight-binding band calculations and magnetic susceptibility measurements. The 2D crystal/electronic structure can be finely modulated by chemical modifications using other octahedral anions or selenized donors,[260,261] while maintaining the isomorphous structure, allowing other novel physical properties to be explored.

4. Conclusions

In this highlight, we presented examples of studies using organic conductors as electrodes to suppress the contact resistance (charge injection barrier) at the OSC–electrode interface of organic transistors. Conductive organic materials have similar chemical properties and surface energies in contrast to inorganic metals. Thus, the contact resistance of organic transistors can be significantly reduced by using organic electrodes, in addition to the use of dopants and SAMs as a buffer layer at the OSC–electrode interface. In particular, the transistor fabrication technique using direct chemical doping, which is the standard for silicon semiconductors, is a unique attempt to develop a new fabrication method for organic devices. The development of high-conductivity organic conductors with organic semiconductors is essential for the widespread application of this technique. New semiconductors that achieve not only high mobility but also air stability and redox activity should be developed. Thienoacene-based CT salts, such as BTBT, which have been developed for this purpose, have the potential to create new trends in research on the physical properties of organic conductors.

Conflicts of interest

There are no conflicts to declare.

Acknowledgements

This work was partly supported by the JSPS KAKENHI Grant Numbers 20K15356, 21K14699 and 23K04882, JST CREST Grant Number JPMJCR18J2, and The Mazda Foundation, Izumi Science and Technology Foundation, Research Foundation for the Electrotechnology of Chubu.

Notes and references

1 D. D. Eley, *Nature*, 1948, **162**, 819–819.
2 H. Akamatu and H. Inokuchi, *J. Chem. Phys.*, 1950, **18**, 810–811.
3 H. Inokuchi, *Bull. Chem. Soc. Jpn.*, 1951, **24**, 222–226.
4 H. Akamatsu, H. Inokuchi and Y. Matsunaga, *Nature*, 1954, **173**, 168–169.
5 T. Naito, *Crystals*, 2021, **11**, 838.
6 T. Naito, *Bull. Chem. Soc. Jpn.*, 2017, **90**, 89–136.
7 R. Kato, *Bull. Chem. Soc. Jpn.*, 2014, **87**, 355–374.
8 F. Wudl, G. M. Smith and E. J. Hufnagel, *Chem. Commun.*, 1970, 1453–1454.
9 D. L. Coffen, *Tetrahedron Lett.*, 1970, 2633–2636.
10 H. Prinzbach, H. Berger and A. Lütringhaus, *Angew. Chem., Int. Ed. Engl.*, 1965, **4**, 435.
11 A. Takamizawa and K. Hirai, *Chem. Pharm. Bull.*, 1969, **17**, 1931–1936.
12 J. Yamada and T. Sugimoto, *TTF Chemistry–Fundamentals and Applications of Tetrathiafulvalene*, Kodansha & Springer, Tokyo, Japan, 2004.
13 Y. Morita, S. Suzuki, K. Sato and T. Takui, *Nat. Chem.*, 2011, **3**, 197–204.
14 Y. Kobayashi, T. Terauchi, S. Sumi and Y. Matsushita, *Nat. Mater.*, 2017, **16**, 109–114.
15 S. K. Pal, P. Bag, M. E. Itkis, F. S. Tham and R. C. Haddon, *J. Am. Chem. Soc.*, 2014, **136**, 14738–14741.
16 A. Mailman, S. M. Winter, X. Yu, C. M. Robertson, W. Yong, J. S. Tse, R. A. Secco, Z. Liu, P. A. Dube, J. A. K. Howard and R. T. Oakley, *J. Am. Chem. Soc.*, 2012, **134**, 9886–9889.
17 J. W. L. Wong, A. Mailman, K. Lekin, S. M. Winter, W. Yong, J. Zhao, S. V. Garimella, J. S. Tse, R. A. Secco, S. Desgreniers, Y. Ohishi, F. Borondics and R. T. Oakley, *J. Am. Chem. Soc.*, 2014, **136**, 1070–1081.
18 S. K. Mandal, S. Samanta, M. E. Itkis, D. W. Jensen, R. W. Reed, R. T. Oakley, F. S. Tham, B. Donnadieu and R. C. Haddon, *J. Am. Chem. Soc.*, 2006, **128**, 1982–1994.
19 S. K. Pal, M. E. Itkis, F. S. Tham, R. W. Reed, R. T. Oakley and R. C. Haddon, *Science*, 2005, **309**, 281–284.
20 Y. Kobayashi, K. Hirata, S. N. Hood, H. Yang, A. Walsh, Y. Matushita and K. Ishioka, *Chem. Sci.*, 2020, **11**, 11699–11704.
21 H. Tanaka, Y. Okano, H. Kobayashi, W. Suzuki and A. Kobayashi, *Science*, 2001, **291**, 285–287.
22 W. Suzuki, E. Fujiwara, A. Kobayashi, Y. Fujishiro, E. Nishibori, M. Tanaka, M. Sakata, H. Fujiwara and H. Kobayashi, *J. Am. Chem. Soc.*, 2003, **125**, 1486–1487.
23 T. Tanaka, H. Kobayashi and A. Kobayashi, *J. Am. Chem. Soc.*, 2002, **124**, 10002–10003.
24 N. Tenn, N. Bellec, O. Jeannin, L. Piekara-Sady, P. Auban-Senzier, J. Iniguez, E. Canadell and D. Lorcy, *J. Am. Chem. Soc.*, 2009, **131**, 16961–16967.
25 H. B. Cui, H. Kobayashi, S. Ishibashi, M. Sasa, F. Iwase, R. Kato and A. Kobayashi, *J. Am. Chem. Soc.*, 2014, **136**, 7619–7622.
26 H. Kamo, A. Ueda, T. Isono, K. Takahashi and H. Mori, *Tetrahedron Lett.*, 2012, **53**, 4385–4388.
27 T. Isono, H. Kamo, A. Ueda, K. Takahashi, A. Nakao, R. Kumai, H. Nakano, K. Kobayashi, Y. Murakami and H. Mori, *Nat. Commun.*, 2013, **4**, 1344.
28 A. Ueda, S. Yamada, T. Isono, H. Kamo, A. Nakao, R. Kumai, H. Nakao, Y. Murakami, K. Yamamoto, Y. Nishio and H. Mori, *J. Am. Chem. Soc.*, 2014, **136**, 12184–12192.
29 H. Mori, S. Yokomori, S. Dekura and A. Ueda, *Chem. Commun.*, 2022, **58**, 5668–5682.
30 A. Ueda, *Bull. Chem. Soc. Jpn.*, 2017, **90**, 1181–1188.
31 B. Kippelen and J. L. Brédas, *Energy Environ. Sci.*, 2009, **2**, 251–261.
32 S. B. Darling and F. You, *RSC Adv.*, 2013, **3**, 17633–17648.
33 Y. Cui, Y. Xu, H. Yao, P. Bi, L. Hong, J. Zhang, Y. Zu, T. Zhang, J. Qin, J. Ren, Z. Chen, C. He, X. Hao, Z. Wei and J. Hou, *Adv. Mater.*, 2021, **33**, 2102420.
34 C. Xu, Z. Zhao, K. Yang, L. Niu, X. Ma, Z. Zhou, X. Zhang and F. Zhang, *J. Mater. Chem. A*, 2022, **10**, 6291–6329.
35 M. Zhang, L. Zhu, G. Zhou, T. Hao, C. Qiu, Z. Zhao, Q. Hu, B. W. Larson, H. Zhu, Z. Ma, Z. Tang, W. Feng, Y. Zhang, T. P. Russell and F. Liu, *Nat. Commun.*, 2021, **12**, 309.

36 L. Zhan, S. Li, X. Xia, Y. Li, X. Lu, L. Zuo, M. Shi and H. Chen, *Adv. Mater.*, 2021, **33**, 2007231.
37 F. Huewe, A. Steeger, K. Kostova, L. Burroughs, I. Bauer, P. Strohriegl, V. Dimitrov, S. Woodward and J. Pflaum, *Adv. Mater.*, 2017, **29**, 1605682.
38 Q. Zhang, Y. Sun, W. Xu and D. Zhu, *Adv. Mater.*, 2014, **26**, 6829–6851.
39 B. Russ, A. Glaudell, J. J. Urban, M. L. Chabinyc and R. A. Segalman, *Nat. Rev. Mater.*, 2016, **1**, 16050.
40 J. Liu, B. V. D. Zee, R. Alessandri, S. Sami, J. Dong, M. I. Nugraha, A. J. Barker, S. Rousseva, L. Qiu, X. Qiu, N. Klasen, R. C. Chiechi, D. Baran, M. Caironi, T. D. Anthopoulos, G. Portale, R. W. A. Havenith, S. J. Marrink, J. C. Hummelen and L. J. A. Koster, *Nat. Commun.*, 2020, **11**, 5694.
41 H. Sirringhaus, *Adv. Mater.*, 2014, **26**, 1319–1335.
42 M. Mas-Torrent and C. Rovira, *Chem. Rev.*, 2011, **111**, 4833–4856.
43 H. Chen, W. Zhang, M. Li, G. He and X. Guo, *Chem. Rev.*, 2020, **120**, 2879–2949.
44 T. Higashino and T. Mori, *Phys. Chem. Chem. Phys.*, 2022, **24**, 9770–9806.
45 W. Tang, Y. Huang, L. Han, R. Liu, Y. Su, X. Guo and F. Yan, *J. Mater. Chem. C*, 2019, **7**, 790–808.
46 T. Mori, *Bull. Chem. Soc. Jpn.*, 2016, **89**, 973–986.
47 C. D. Dimitrakopoulos and P. R. L. Malenfant, *Adv. Mater.*, 2002, **14**, 99–117.
48 J. Takeya, K. Yamada, K. Hara, K. Shigeto, K. Tsukagoshi, S. Ikehata and Y. Aoyagi, *Appl. Phys. Lett.*, 2006, **88**, 112102.
49 H. Shimotani, H. Asanuma, J. Takeya and Y. Iwasa, *Appl. Phys. Lett.*, 2006, **89**, 203501.
50 J. Lee, M. J. Panzer, Y. He, T. P. Lodge and C. D. Frisbie, *J. Am. Chem. Soc.*, 2007, **129**, 4532–4533.
51 R. Misra, M. McCarthy and A. F. Hebard, *Appl. Phys. Lett.*, 2007, **90**, 052905.
52 J. H. Cho, J. Lee, Y. Xia, B. Kim, Y. He, M. J. Renn, T. P. Lodge and C. D. Frisbie, *Nat. Mater.*, 2008, **7**, 900–906.
53 H. M. Yamamoto, M. Nakano, M. Suda, Y. Iwasa, M. Kawasaki and R. Kato, *Nat. Commun.*, 2013, **4**, 2379.
54 M. Suda and H. M. Yamamoto, *Phys. Chem. Chem. Phys.*, 2018, **20**, 1321–1331.
55 H. M. Yamamoto, *Bull. Chem. Soc. Jpn.*, 2021, **94**, 2505–2539.
56 M. Waldrip, O. D. Jurchescu, D. J. Gundlach and E. G. Bittle, *Adv. Funct. Mater.*, 2020, **30**, 1904576.
57 C. Liu, G. Li, R. D. Pietro, J. Huang, Y. Y. Noh, X. Liu and T. Minari, *Phys. Rev. Appl.*, 2017, **8**, 034020.
58 D. Natali and M. Caironi, *Adv. Mater.*, 2012, **24**, 1357–1387.
59 S. M. Sze and K. K. Ng, *Physics of Semiconductor Devices*, John Wiley & Sons, Inc., Hoboken, New Jersey, 3rd edn, 2007.
60 H. Wada, K. Shibata, Y. Bando and T. Mori, *J. Mater. Chem.*, 2008, **18**, 4165–4171.
61 H. Ishii, K. Sugiyama, E. Ito and K. Seki, *Adv. Mater.*, 1999, **11**, 605–625.
62 H. Ishii and K. Seki, *IEEE Trans. Electron Devices*, 1997, **44**, 1295.
63 H. Ishii, K. Sugiyama, D. Yoshimura, E. Ito, Y. Ouchi and K. Seki, *IEEE J. Sel. Top. Quantum Electron.*, 1998, **4**, 24.
64 G. Hill and A. Kahn, Interface electronic properties of organic molecular semiconductors, Organic Light-Emitting Materials and Devices II, *Proc. SPIE 3476*, 1998.
65 K. Shibata, K. Ishikawa, H. Takezoe, H. Wada and T. Mori, *Appl. Phys. Lett.*, 2008, **92**, 023305.
66 E. H. Rhoderick and R. H. Williams, *Metal-Semiconductor Contacts*, Clarendon, Oxford, 2nd edn, 1988.
67 T. Minari, P. Darmawan, C. Liu, Y. Li, Y. Xu and K. Tsukagoshi, *Appl. Phys. Lett.*, 2012, **100**, 093303.
68 Y. Abe, T. Hasegawa, Y. Takahashi, T. Yamada and Y. Tokura, *Appl. Phys. Lett.*, 2005, **87**, 153506.
69 J. Soeda, Y. Hirose, M. Yamagishi, A. Nakao, T. Uemura, K. Nakayama, M. Uno, Y. Nakazawa, K. Takimiya and J. Takeya, *Adv. Mater.*, 2011, **23**, 3309–3314.
70 A. Nollau, M. Pfeiffer, T. Fritz and K. Leo, *J. Appl. Phys.*, 2000, **87**, 4340–4347.
71 J. H. Oh, P. Wei and Z. Bao, *Appl. Phys. Lett.*, 2010, **97**, 243305.
72 B. D. Naab, S. Guo, S. Olthof, E. G. B. Evans, P. Wei, G. L. Millhauser, A. Kahn, S. Barlow, S. R. Marder and Z. Bao, *J. Am. Chem. Soc.*, 2013, **135**, 15018–15025.
73 P. Wei, J. H. Oh, G. Dong and Z. Bao, *J. Am. Chem. Soc.*, 2010, **132**, 8852–8853.
74 B. D. Naab, S. Himmelberger, Y. Diao, K. Vandewal, P. Wei, B. Lussem, A. Salleo and Z. Bao, *Adv. Mater.*, 2013, **25**, 4663–4667.
75 J. T. E. Quinn, J. Zhu, X. Li, J. Wang and Y. Li, *J. Mater. Chem. C*, 2017, **5**, 8654–8681.
76 B. de Boer, A. Hadipour, M. M. Mandoc, T. van Woudenbergh and P. W. M. Blom, *Adv. Mater.*, 2005, **17**, 621–625.
77 S. Tatara, Y. Kuzumoto and M. Kitamura, *Jpn. J. Appl. Phys.*, 2016, **55**, 03DD02.
78 K. Aoshima, S. Arai, K. Fukuhara, T. Yamada and T. Hasegawa, *Org. Electron.*, 2017, **41**, 137–142.
79 G. Kitahara, K. Aoshima, J. Tsutsumi, H. Minemawari, S. Arai and T. Hasegawa, *Org. Electron.*, 2017, **50**, 426–428.
80 Y. Yu, M. Kanno, H. Wada, Y. Bando, M. Ashizawa, A. Tanioka and T. Mori, *Phys. B*, 2010, **405**, S378–S380.
81 T. Matsushima, Y. Kinoshita and H. Murata, *Appl. Phys. Lett.*, 2007, **91**, 253504–253506.
82 T. Kadoya, O. Pitayatanakul and T. Mori, *Org. Electron.*, 2015, **21**, 106–110.
83 K. Shibata, H. Wada, K. Ishikawa, H. Takezoe and T. Mori, *Appl. Phys. Lett.*, 2007, **90**, 193509.
84 J. Ferraris, D. O. Cowan, V. Walatka and J. H. Perlstein, *J. Am. Chem. Soc.*, 1973, **95**, 948–949.
85 L. B. Coleman, M. J. Cohen, D. J. Sandman, F. G. Yamagishi, A. F. Garito and A. J. Heeger, *Solid State Commun.*, 1993, **88**, 989–995.
86 T. E. Phillips, T. J. Kistenmacher, J. P. Ferraris and D. O. Cowan, *J. Chem. Soc., Chem. Commun.*, 1973, 471–472.

87 Y. Takahashi, T. Hasegawa, Y. Abe, Y. Tokura, K. Nishimura and G. Saito, *Appl. Phys. Lett.*, 2005, **86**, 063504.
88 Y. Takahashi, T. Hasegawa, Y. Abe, Y. Tokura and G. Saito, *Appl. Phys. Lett.*, 2006, **88**, 073504.
89 D. de Caro, K. Jacob, H. Hahioui, C. Faulmann, L. Valade, T. Kadoya, T. Mori, J. Fraxedas and L. Viau, *New J. Chem.*, 2011, **35**, 1315–1319.
90 T. Kadoya, D. de Caro, K. Jacob, C. Faulmann, L. Valade and T. Mori, *J. Mater. Chem.*, 2011, **21**, 18421–18424.
91 H. Wada and T. Mori, *Appl. Phys. Lett.*, 2008, **93**, 213303.
92 H. Wada and T. Mori, *Appl. Phys. Lett.*, 2009, **95**, 253307.
93 T. Mori, *Chem. Lett.*, 2011, **40**, 428–434.
94 R. Srinivasan and B. Braren, *Chem. Rev.*, 1989, **89**, 1303–1316.
95 F. Raimondi, S. Abolhassani, R. Brütsch, F. Geiger, T. Lippert, J. Wambach, J. Wei and A. Wokaun, *J. Appl. Phys.*, 2000, **88**, 3659.
96 J. Inoue, H. Wada and T. Mori, *Jpn. J. Appl. Phys.*, 2010, **49**, 071605.
97 S. Tamura, T. Kadoya, T. Kawamoto and T. Mori, *Appl. Phys. Lett.*, 2013, **102**, 063305.
98 S. Tamura, T. Kadoya and T. Mori, *Appl. Phys. Lett.*, 2014, **105**, 023301.
99 T. Kadoya, S. Tamura and T. Mori, *J. Phys. Chem. C*, 2014, **118**, 23139–23146.
100 C. Rovira, *Chem. Rev.*, 2004, **104**, 5289–5317.
101 H. Jiang, X. Yang, Z. Cui, Y. Liu, H. Li, W. Hu and C. Kloc, *CrystEngComm*, 2014, **16**, 5968–5983.
102 R. Pfattner, S. T. Bromley, C. Rovira and M. Mas-Torrent, *Adv. Funct. Mater.*, 2016, **26**, 2256–2275.
103 M. Kanno, Y. Bando, T. Shirahata, J. Inoue, H. Wada and T. Mori, *J. Mater. Chem.*, 2009, **19**, 6548–6555.
104 J. Inoue, M. Kanno, M. Ashizawa, C. Seo, A. Tanioka and T. Mori, *Chem. Lett.*, 2010, **39**, 538–540.
105 J. Nagakubo, M. Ashizawa, T. Kawamoto, A. Tanioka and T. Mori, *Phys. Chem. Chem. Phys.*, 2011, **13**, 14370–14377.
106 T. Higashino, Y. Akiyama, H. Kojima, T. Kawamoto and T. Mori, *Crystals*, 2012, **2**, 1222–1238.
107 L. Alcacer and A. H. Maki, *J. Phys. Chem.*, 1974, **78**, 215–217.
108 H. J. Keller, D. Nöthe, H. Pritzkow, D. Wehe, M. Werner, P. Koch and D. Schweitzer, *Mol. Cryst. Liq. Cryst.*, 1980, **62**, 181–199.
109 P. Koch, D. Schweitzer, R. H. Harms, H. J. Keller, H. Schäfer, H. W. Helberg, R. Wilckens, H. P. Geserich and W. Ruppel, *Mol. Cryst. Liq. Cryst.*, 1982, **86**, 87–101.
110 D. Schweitzer, I. Hennig, K. Bender, H. Endres and H. J. Keller, *Mol. Cryst. Liq. Cryst.*, 1985, **120**, 213–220.
111 V. Gama, M. Almeida, R. T. Henriques, I. C. Santos, A. Domingos, S. Ravy and J. P. Pouget, *J. Phys. Chem.*, 1991, **95**, 4263–4267.
112 V. Gama, R. Henriques, M. Almeida and L. Alcácer, *Synth. Met.*, 1991, **42**, 2553–2556.
113 C. Kröhnke, V. Enkelmann and G. Wegner, *Angew. Chem., Int. Ed. Engl.*, 1980, **19**, 912–919.
114 H. Eichele, M. Schwoerer, C. Kröhnke and G. Wegner, *Chem. Phys. Lett.*, 1981, **77**, 311–313.
115 V. Enkelmann, B. S. Morra, C. Kröhnke, G. Wegner and J. Heinze, *Chem. Phys.*, 1982, **66**, 303–313.
116 E. Dormann and G. Sachs, *Ber. Bunsen-Ges.*, 1987, **91**, 879–885.
117 K. Bechgaard, *Mol. Cryst. Liq. Cryst.*, 1985, **125**, 81–89.
118 N. Thorup, G. Rindorf, C. S. Jacobsen, K. Bechgaard, I. Johannsen and K. Mortensen, *Mol. Cryst. Liq. Cryst.*, 1985, **120**, 349–352.
119 K. Nakasuji, H. Kubota, T. Kotani, I. Murata, G. Saito, T. Enoki, K. Imaeda, H. Inokuchi, M. Honda, C. Katayama and J. Tanaka, *J. Am. Chem. Soc.*, 1986, **108**, 3460–3466.
120 K. Nakasuji, M. Sasaki, T. Kotani, I. Murata, T. Enoki, K. Imaeda, H. Inokuchi, A. Kawamoto and J. Tanaka, *J. Am. Chem. Soc.*, 1987, **109**, 6970–6975.
121 A. Kawamoto, J. Tanaka, A. Oda, H. Mizumura, I. Murata and K. Nakasuji, *Bull. Chem. Soc. Jpn.*, 1990, **63**, 2137–2145.
122 Y. Morita, Y. Yakiyama, T. Murata and K. Nakasuji, *Solid State Sci.*, 2008, **10**, 1720–1723.
123 J. Bendix, K. Bechgaard and J. B. Christensen, *RSC Adv.*, 2021, **11**, 14607–14614.
124 Y. Matsunaga, *J. Chem. Phys.*, 1965, **42**, 2248–2249.
125 E. A. Perez-Albuerne, H. Johnson and D. J. Trevoy, *J. Chem. Phys.*, 1971, **55**, 1547–1554.
126 L. I. Buravov, G. I. Zvereva, V. F. Kaminskii, L. P. Rosenberg, M. L. Khidekel, R. P. Shibaeva, I. F. Shchegolev and E. B. Yagubskii, *J. Chem. Soc., Chem. Commun.*, 1976, 720–721.
127 L. C. Isett and E. A. Perez-Albuerne, *Solid State Commun.*, 1977, **21**, 433–435.
128 T. Inabe and Y. Matsunaga, *Bull. Chem. Soc. Jpn.*, 1978, **51**, 2813–2816.
129 Y. Matsunaga and K. Takayanagi, *Bull. Chem. Soc. Jpn.*, 1980, **53**, 2796–2799.
130 P. Kathirgamanathan and D. R. Rosseinsky, *J. Chem. Soc., Chem. Commun.*, 1980, 356.
131 H. Tanaka, T. Nogami and H. Mikawa, *Chem. Lett.*, 1982, **11**, 727–730.
132 T. Nogami, H. Tanaka, S. Ohnishi, Y. Tasaka and H. Mikawa, *Bull. Chem. Soc. Jpn.*, 1984, **57**, 22–25.
133 K. Takimiya, H. Miyamoto, Y. Aso, T. Otsubo and F. Ogura, *Chem. Lett.*, 1990, **19**, 567–570.
134 K. Takimiya, Y. Aso, T. Otsubo and F. Ogura, *Bull. Chem. Soc. Jpn.*, 1991, **64**, 2091–2102.
135 K. Takimiya, A. Ohnishi, Y. Aso, T. Otsubo, F. Ogura, K. Kawabata, K. Tanaka and M. Mizutani, *Bull. Chem. Soc. Jpn.*, 1994, **67**, 766–772.
136 T. Otsubo, K. Takimiya and Y. Aso, *Phosphorus, Sulfur Silicon Relat. Elem.*, 1998, **136**, 447–462.
137 T. Ohta, T. Nagano, K. Ochi, Y. Kubozono and A. Fujiwara, *Appl. Phys. Lett.*, 2006, **88**, 103506.
138 J.-W. Lee, H.-S. Kang, M.-K. Kim, K. Kim, M.-Y. Cho, Y.-W. Kwon, J. Joo, J.-I. Kim and C.-S. Hong, *J. Appl. Phys.*, 2007, **102**, 124104.

139 H. Jiang, K. K. Zhang, J. Ye, F. Wei, P. Hu, J. Guo, C. Liang, X. Chen, Y. Zhao, L. E. McNeil, W. Hu and C. Kloc, *Small*, 2013, **9**, 990–995.
140 C.-T. Hsieh, C.-Y. Chen, H.-Y. Lin, C.-J. Yang, T.-J. Chen, K.-Y. Wu and C.-L. Wang, *J. Phys. Chem. C*, 2018, **122**, 16242–16248.
141 A. L. Briseno, Q. Miao, M.-M. Ling, C. Reese, H. Meng, Z. Bao and F. Wudl, *J. Am. Chem. Soc.*, 2006, **128**, 15576–15577.
142 A. L. Briseno, S. C. B. Mannsfeld, X. Lu, Y. Xiong, S. A. Jenekhe, Z. Bao and Y. Xia, *Nano Lett.*, 2007, **7**, 668–675.
143 S. Wen, A. Li, J. Song, W. Deng, K. Han and W. A. Goddard, *J. Phys. Chem. B*, 2009, **113**, 8813–8819.
144 L. Zhang, S. M. Fakhouri, F. Liu, J. C. Timmons, N. A. Ran and A. L. Briseno, *J. Mater. Chem.*, 2011, **21**, 1329–1337.
145 K. Takimiya, H. Ebata, K. Sakamoto, T. Izawa, T. Otsubo and Y. Kunugi, *J. Am. Chem. Soc.*, 2006, **128**, 12604–12605.
146 H. Ebata, T. Izawa, E. Miyazaki, K. Takimiya, M. Ikeda, H. Kuwabara and T. Yui, *J. Am. Chem. Soc.*, 2007, **129**, 15732–15733.
147 H. Minemawari, T. Yamada, H. Matsui, J. Tsutsumi, S. Haas, R. Chiba, R. Kumai and T. Hasegawa, *Nature*, 2011, **475**, 364–367.
148 K. Takimiya, S. Shinamura, I. Osaka and E. Miyazaki, *Adv. Mater.*, 2011, **23**, 4347–4370.
149 A. Y. Amin, A. Khassanov, K. Reuter, T. Meyer-Friedrichsen and M. Halik, *J. Am. Chem. Soc.*, 2012, **134**, 16548–16550.
150 T. Schmaltz, A. Y. Amin, A. Khassanov, T. Meyer-Friedrichsen, H.-G. G. Steinrück, A. Magerl, J. J. Segura, K. Voitchovsky, F. Stellacci and M. Halik, *Adv. Mater.*, 2013, **25**, 4511–4514.
151 V. S. Vyas, R. Gutzler, J. Nuss, K. Kern and B. V. Lotsch, *CrystEngComm*, 2014, **16**, 7389–7392.
152 H. Iino, T. Usui and J.-I. Hanna, *Nat. Commun.*, 2015, **6**, 6828.
153 G. Schweicher, V. Lemaur, C. Niebel, C. Ruzié, Y. Diao, O. Goto, W. Lee, Y. Kim, J. Arlin, J. Karpinska, A. R. Kennedy, S. R. Parkin, Y. Olivier, S. C. B. B. Mannsfeld, J. Cornil, Y. H. Geerts and Z. Bao, *Adv. Mater.*, 2015, **27**, 3066–3072.
154 J.-M. Cho, T. Higashino and T. Mori, *Appl. Phys. Lett.*, 2015, **106**, 193303.
155 C. Niebel, Y. Kim, C. Ruzié, J. Karpinska, B. Chattopadhyay, G. Schweicher, A. Richard, V. Lemaur, Y. Olivier, J. Cornil, A. R. Kennedy, Y. Diao, W.-Y. Y. Lee, S. Mannsfeld, Z. Bao and Y. H. Geerts, *J. Mater. Chem. C*, 2015, **3**, 674–685.
156 Y. He, M. Sezen, D. Zhang, A. Li, L. Yan, H. Yu, C. He, O. Goto, Y.-L. L. Loo and H. Meng, *Adv. Electron. Mater.*, 2016, **2**, 1600179.
157 K. He, W. Li, H. Tian, J. Zhang, D. Yan, Y. Geng and F. Wang, *ACS Appl. Mater. Interfaces*, 2017, **9**, 35427–35436.
158 S. Arai, S. Inoue, T. Hamai, R. Kumai and T. Hasegawa, *Adv. Mater.*, 2018, **30**, 1707256.
159 T. Higashino, A. Ueda and H. Mori, *New J. Chem.*, 2019, **43**, 884–892.
160 T. Kadoya, S. Mano, A. Hori, K. Tahara, K. Sugimoto, K. Kubo, M. Abe, H. Tajima and J. Yamada, *Org. Electron.*, 2020, **78**, 105570.
161 S. Inoue, K. Nikaido, T. Higashino, S. Arai, M. Tanaka, R. Kumai, S. Tsuzuki, S. Horiuchi, H. Sugiyama, Y. Segawa, K. Takaba, S. Maki-Yonekura, K. Yonekura and T. Hasegawa, *Chem. Mater.*, 2022, **34**, 72–83.
162 K. Nikaido, S. Inoue, R. Kumai, T. Higashino, S. Matsuoka, S. Arai and T. Hasegawa, *Adv. Mater. Interfaces*, 2022, **9**, 2201789.
163 R. Akai, K. Oka, S. Dekura, H. Mori and N. Tohnai, *Bull. Chem. Soc. Jpn.*, 2022, **95**, 1178–1182.
164 T. Yasuda, T. Doto, K. Fujita and T. Tsutsui, *Mol. Cryst. Liq. Cryst.*, 2006, **444**, 219–224.
165 T. Kadoya, M. Ashizawa, T. Higashino, T. Kawamoto, S. Kumeta, H. Matsumoto and T. Mori, *Phys. Chem. Chem. Phys.*, 2013, **15**, 17818–17822.
166 Y. Kiyota, T. Kadoya, K. Yamamoto, K. Iijima, T. Higashino, T. Kawamoto, K. Takimiya and T. Mori, *J. Am. Chem. Soc.*, 2016, **138**, 3920–3925.
167 T. Higashino, T. Kadoya, S. Kumeta, K. Kurata, T. Kawamoto and T. Mori, *Eur. J. Inorg. Chem.*, 2014, 3895–3898.
168 T. Kadoya, R. Oki, Y. Kiyota, Y. Koyama, T. Higashino, K. Kubo, T. Mori and J. Yamada, *J. Phys. Chem. C*, 2019, **123**, 5216–5221.
169 E. M. Engler and V. V. Patel, *J. Am. Chem. Soc.*, 1974, **96**, 7376–7378.
170 S. Etemad, *Phys. Rev. B*, 1976, **13**, 2254–2261.
171 D. Jérome, A. Mazaud, M. Ribault and K. Bechgaard, *J. Phys. Lett.*, 1980, **41**, 95–98.
172 R. L. Greene and E. M. Engler, *Phys. Rev. Lett.*, 1980, **45**, 1587–1590.
173 M. D. Mays, R. D. McCullough, D. O. Cowan, T. O. Poehler, W. A. Bryden and T. J. Kistenmacher, *Solid State Commun.*, 1988, **65**, 1089–1092.
174 T. Higashino, A. Ueda, J. Yoshida and H. Mori, *Chem. Commun.*, 2017, **53**, 3426–3429.
175 J. Cornil, D. Beljonne and J. L. Brédas, *J. Chem. Phys.*, 1995, **103**, 842–849.
176 D. Beljonne, J. Cornil, R. H. Friend, R. A. J. Janssen and J. L. Brédas, *J. Am. Chem. Soc.*, 1996, **118**, 6453–6461.
177 T. Okamoto, K. Kudoh, A. Wakamiya and S. Yamaguchi, *Chem. – Eur. J.*, 2007, **13**, 548–556.
178 S. S. Zade, N. Zamoshchik and M. Bendikov, *Chem. – Eur. J.*, 2009, **15**, 8613–8624.
179 H. Méndez, G. Heimel, A. Opitz, K. Sauer, P. Barkowski, M. Oehzelt, J. Soeda, T. Okamoto, J. Takeya, J. B. Arlin, J. Y. Balandier, Y. Geerts, N. Koch and I. Salzmann, *Angew. Chem., Int. Ed.*, 2013, **52**, 7751–7755.
180 J. Tsutsumi, S. Matsuoka, S. Inoue, H. Minemawari, T. Yamada and T. Hasegawa, *J. Mater. Chem. C*, 2015, **3**, 1976–1981.
181 Y. Shibata, J. Tsutsumi, S. Matsuoka, K. Matsubara, Y. Yoshida, M. Chikamatsu and T. Hasegawa, *Appl. Phys. Lett.*, 2015, **106**, 143303.

182 Y. Shibata, J. Tsutsumi, S. Matsuoka, H. Minemawari, S. Arai, R. Kumai and T. Hasegawa, *Adv. Electron. Mater.*, 2017, **3**, 1700097.
183 H. Koike, J. Tsutsumi, S. Matsuoka, K. Sato, T. Hasegawa and K. Kanai, *Org. Electron.*, 2016, **39**, 184–190.
184 L. Zhu, H. Geng, Y. Yi and Z. Wei, *Phys. Chem. Chem. Phys.*, 2017, **19**, 4418–4425.
185 K. Iijima, R. Sanada, D. Yoo, R. Sato, T. Kawamoto and T. Mori, *ACS Appl. Mater. Interfaces*, 2018, **10**, 10262–10269.
186 R. Sato, T. Kawamoto and T. Mori, *J. Mater. Chem. C*, 2019, **7**, 567–577.
187 H. Geng, L. Zhu, Y. Yi, D. Zhu and Z. Shuai, *Chem. Mater.*, 2019, **31**, 6424–6434.
188 Q. Wei, L. Liu, S. Xiong, X. Zhang, W. Deng, X. Zhang and J. Jie, *J. Phys. Chem. Lett.*, 2020, **11**, 359–365.
189 S. Takamaru, J. Hanna and H. Iino, *Appl. Phys. Express*, 2022, **15**, 031001.
190 R. Sato, M. Dogishi, T. Higashino, T. Kadoya, T. Kawamoto and T. Mori, *J. Phys. Chem. C*, 2017, **121**, 6561–6568.
191 N. Castagnetti, A. Girlando, M. Masino, C. Rizzoli and C. Rovira, *Cryst. Growth Des.*, 2017, **17**, 6255–6261.
192 R. R. Dasari, X. Wang, R. A. Wiscons, H. F. Haneef, A. Ashokan, Y. Zhang, M. S. Fonari, S. Barlow, V. Coropceanu, T. V. Timofeeva, O. D. Jurchescu, J. Brédas, A. J. Matzger and S. R. Marder, *Adv. Funct. Mater.*, 2019, **29**, 1904858.
193 A. Ashokan, C. Hanson, N. Corbin, J.-L. Brédas and V. Coropceanu, *Mater. Chem. Front.*, 2020, **4**, 3623–3631.
194 J. Zhang, J. Jin, H. Xu, Q. Zhang and W. Huang, *J. Mater. Chem. C*, 2018, **6**, 3485–3498.
195 A. A. Dar and S. Rashid, *CrystEngComm*, 2021, **23**, 8007–8026.
196 W. Wang, L. Luo, P. Sheng, J. Zhang and Q. Zhang, *Chem. – Eur. J.*, 2021, **27**, 464–490.
197 T. Higashino, M. Dogishi, T. Kadoya, R. Sato, T. Kawamoto and T. Mori, *J. Mater. Chem. C*, 2016, **4**, 5981–5987.
198 L. Fijahi, T. Salzillo, A. Tamayo, M. Bardini, C. Ruzié, C. Quarti, D. Beljonne, S. D'Agostino, Y. H. Geerts and M. Mas-Torrent, *J. Mater. Chem. C*, 2022, **10**, 7319–7328.
199 S. Matsuoka, K. Ogawa, R. Ono, K. Nikaido, S. Inoue, T. Higashino, M. Tanaka, J. Tsutsumi, R. Kondo, R. Kumai, S. Tsuzuki, S. Arai and T. Hasegawa, *J. Mater. Chem. C*, 2022, **10**, 16471–16479.
200 M. Mizuno, A. F. Garito and M. P. Cava, *J. Chem. Soc., Chem. Commun.*, 1978, 18–19.
201 G. Saito, T. Enoki, K. Toriumi and H. Inokuchi, *Solid State Commun.*, 1982, **42**, 557–560.
202 T. Mori, A. Kobayashi, Y. Sasaki, H. Kobayashi, G. Saito and H. Inokuchi, *Chem. Lett.*, 1982, **11**, 1963–1966.
203 S. S. P. Parkin, E. M. Engler, R. R. Schumaker, R. Lagier, V. Y. Lee, J. C. Scott and R. L. Greene, *Phys. Rev. Lett.*, 1983, **50**, 270–273.
204 E. B. Yagubskii, I. F. Shchegolev, V. N. Laukhin, P. A. Kononovich, M. V. Karatsovnik, A. V. Zvarykina and L. I. Buravov, *JETP Lett.*, 1984, **39**, 12–16.
205 T. Mori, A. Kobayashi, Y. Sasaki, H. Kobayashi, G. Saito and H. Inokuchi, *Chem. Lett.*, 1984, **13**, 957–960.
206 T. Mori, A. Kobayashi, Y. Sasaki, H. Kobayashi, G. Saito and H. Inokuchi, *Bull. Chem. Soc. Jpn.*, 1984, **57**, 627–633.
207 H. Kobayashi, R. Kato, A. Kobayashi, Y. Nishio, K. Kajita and W. Sasaki, *Chem. Lett.*, 1986, **15**, 789–792.
208 H. Kobayashi, R. Kato, A. Kobayashi, Y. Nishio, K. Kajita and W. Sasaki, *Chem. Lett.*, 1986, **15**, 833–836.
209 R. Kato, H. Kobayashi, A. Kobayashi, S. Moriyama, Y. Nishio, K. Kajita and W. Sasaki, *Chem. Lett.*, 1987, **16**, 507–510.
210 A. Kobayashi, R. Kato, H. Kobayashi, S. Moriyama, Y. Nishio, K. Kajita and W. Sasaki, *Chem. Lett.*, 1987, **16**, 459–462.
211 C. Hotta, *J. Phys. Soc. Jpn.*, 2003, **72**, 840–853.
212 T. Mori, *Bull. Chem. Soc. Jpn.*, 1998, **71**, 2509–2526.
213 T. Mori, H. Mori and S. Tanaka, *Bull. Chem. Soc. Jpn.*, 1999, **72**, 179–197.
214 T. Mori, *Bull. Chem. Soc. Jpn.*, 1999, **72**, 2011–2027.
215 H. Kobayashi, A. Kobayashi, G. Saito, T. Enoki and H. Inokuchi, *J. Am. Chem. Soc.*, 1983, **105**, 297–298.
216 H. Kobayashi, T. Mori, R. Kato, A. Kobayashi, Y. Sasaki, G. Saito and H. Inokuchi, *Chem. Lett.*, 1983, **12**, 581–584.
217 H. Kobayashi, R. Kato, T. Mori, A. Kobayashi, Y. Sasaki, G. Saito and H. Inokuchi, *Chem. Lett.*, 1983, **12**, 759–762.
218 H. Kobayashi, R. Kato, T. Mori, A. Kobayashi, Y. Sasaki, G. Saito, T. Enoki and H. Inokuchi, *Mol. Cryst. Liq. Cryst.*, 1984, **107**, 33–43.
219 A. Miyazaki, T. Enoki and G. Saito, *Synth. Met.*, 1995, **70**, 793–794.
220 H. Mori, *J. Phys. Soc. Jpn.*, 2006, **75**, 051003.
221 G. Saito and Y. Yoshida, *Chem. Rec.*, 2011, **11**, 124–145.
222 H. Urayama, H. Yamochi, G. Saito, K. Nozawa, T. Sugano, M. Kinoshita, S. Sato, K. Oshima, A. Kawamoto and J. Tanaka, *Chem. Lett.*, 1988, **17**, 55–58.
223 A. M. Kini, U. Geiser, H. H. Wang, K. D. Carlson, J. M. Williams, W. K. Kwok, K. G. Vandervoort, J. E. Thompson and D. L. Stupka, *Inorg. Chem.*, 1990, **29**, 2555–2557.
224 H. Yamochi, T. Nakamura, T. Komatso, N. Matsukawa, T. Inoue, G. Saito, T. Mori, M. Kusunoki and K. Sakaguchi, *Solid State Commun.*, 1992, **82**, 101–105.
225 J. A. Schlueter, K. D. Carlson, U. Geiser, H. H. Wang, J. M. Williams, W.-K. Kwok, J. A. Fendrich, U. Welp, P. M. Keane, J. D. Dudek, A. S. Komosa, D. Naumann, T. Roy, J. E. Schirber, W. R. Bayless and B. Dodrill, *Phys. C*, 1994, **233**, 379–386.
226 H. Taniguchi, M. Miyashita, K. Uchiyama, K. Satoh, N. Môri, H. Okamoto, K. Miyagawa, K. Kanoda, M. Hedo and Y. Uwatoko, *J. Phys. Soc. Jpn.*, 2003, **72**, 468–471.
227 T. Kawamoto, T. Mori, A. Nakao, Y. Murakami and J. A. Schlueter, *J. Phys. Soc. Jpn.*, 2012, **81**, 023705.
228 F. Sawano, I. Terasaki, H. Mori, T. Mori, M. Watanabe, N. Ikeda, Y. Nogami and Y. Noda, *Nature*, 2005, **437**, 522–524.
229 T. Mori, I. Terasaki and H. Mori, *J. Mater. Chem.*, 2007, **17**, 4343.
230 F. Kagawa, T. Sato, K. Miyagawa, K. Kanoda, Y. Tokura, K. Kobayashi, R. Kumai and Y. Murakami, *Nat. Phys.*, 2013, **9**, 419–422.

231 T. Mori, *Phys. Rev. B*, 2016, **93**, 245104.
232 S. Sasaki, K. Hashimoto, R. Kobayashi, K. Itoh, S. Iguchi, Y. Nishio, Y. Ikemoto, T. Moriwaki, N. Yoneyama, M. Watanabe, A. Ueda, H. Mori, K. Kobayashi, R. Kumai, Y. Murakami, J. Müller and T. Sasaki, *Science*, 2017, **357**, 1381–1385.
233 H. Ito, T. Ishiguro, M. Kubota and G. Saito, *J. Phys. Soc. Jpn.*, 1996, **65**, 2987–2993.
234 K. Kanoda, *Hyperfine Interact.*, 1997, **104**, 235–249.
235 S. Lefebvre, P. Wzietek, S. Brown, C. Bourbonnais, D. Jérome, C. Mézière, M. Fourmigué and P. Batail, *Phys. Rev. Lett.*, 2000, **85**, 5420–5423.
236 H. Mori, M. Kamiya, M. Haemori, H. Suzuki, S. Tanaka, Y. Nishio, K. Kajita and H. Moriyama, *J. Am. Chem. Soc.*, 2002, **124**, 1251–1260.
237 T. Kawamoto, K. Kurata and T. Mori, *J. Phys. Soc. Jpn.*, 2018, **87**, 083703.
238 K. Kajita, T. Ojiro, H. Fujii, Y. Nishio, H. Kobayashi, A. Kobayashi and R. Kato, *J. Phys. Soc. Jpn.*, 1992, **61**, 23–26.
239 N. Tajima, M. Tamura, Y. Nishio, K. Kajita and Y. Iye, *J. Phys. Soc. Jpn.*, 2000, **69**, 543–551.
240 S. Katayama, A. Kobayashi and Y. Suzumura, *J. Phys. Soc. Jpn.*, 2006, **75**, 054705.
241 N. Tajima, S. Sugawara, R. Kato, Y. Nishio and K. Kajita, *Phys. Rev. Lett.*, 2009, **102**, 176403.
242 T. Mori, *J. Phys. Soc. Jpn.*, 2013, **82**, 034712.
243 K. Kajita, Y. Nishio, N. Tajima, Y. Suzumura and A. Kobayashi, *J. Phys. Soc. Jpn.*, 2014, **83**, 072002.
244 R. Kato, H. Cui, T. Tsumuraya, T. Miyazaki and Y. Suzumura, *J. Am. Chem. Soc.*, 2017, **139**, 1770–1773.
245 M. Tamura and R. Kato, *J. Phys.: Condens. Matter*, 2002, **14**, L729–L734.
246 Y. Shimizu, K. Miyagawa, K. Kanoda, M. Maesato and G. Saito, *Phys. Rev. Lett.*, 2003, **91**, 107001.
247 T. Itou, A. Oyamada, S. Maegawa, M. Tamura and R. Kato, *Phys. Rev. B*, 2008, **77**, 104413.
248 T. Isono, H. Kamo, A. Ueda, K. Takahashi, M. Kimata, H. Tajima, S. Tsuchiya, T. Terashima, S. Uji and H. Mori, *Phys. Rev. Lett.*, 2014, **112**, 177201.
249 Y. Shimizu, T. Hiramatsu, M. Maesato, A. Otsuka, H. Yamochi, A. Ono, M. Itoh, M. Yoshida, M. Takigawa, Y. Yoshida and G. Saito, *Phys. Rev. Lett.*, 2016, **117**, 107203.
250 T. Hiramatsu, Y. Yoshida, G. Saito, A. Otsuka, H. Yamochi, M. Maesato, Y. Shimizu, H. Ito, Y. Nakamura, H. Kishida, M. Watanabe and R. Kumai, *Bull. Chem. Soc. Jpn.*, 2017, **90**, 1073–1082.
251 M. Shimozawa, K. Hashimoto, A. Ueda, Y. Suzuki, K. Sugii, S. Yamada, Y. Imai, R. Kobayashi, K. Itoh, S. Iguchi, M. Naka, S. Ishihara, H. Mori, T. Sasaki and M. Yamashita, *Nat. Commun.*, 2017, **8**, 1821.
252 Y. Zhou, K. Kanoda and T.-K. Ng, *Rev. Mod. Phys.*, 2017, **89**, 025003.
253 T. Kadoya, S. Sugiura, K. Tahara, T. Higashino, K. Kubo, T. Sasaki, K. Takimiya and J. Yamada, *CrystEngComm*, 2020, **22**, 5949–5953.
254 C. Wang, H. Nakamura, H. Sugino and K. Takimiya, *J. Mater. Chem. C*, 2018, **6**, 3604–3612.
255 V. Podzorov, S. E. Sysoev, E. Loginova, V. M. Pudalov and M. E. Gershenson, *Appl. Phys. Lett.*, 2003, **83**, 3504–3506.
256 V. Podzorov, E. Menard, A. Borissov, V. Kiryukhin, J. A. Rogers and M. E. Gershenson, *Phys. Rev. Lett.*, 2004, **93**, 086602.
257 J. Takeya, M. Yamagishi, Y. Tominari, R. Hirahara, Y. Nakazawa, T. Nishikawa, T. Kawase, T. Shimoda and S. Ogawa, *Appl. Phys. Lett.*, 2007, **90**, 102120.
258 C. Reese and Z. Bao, *Adv. Mater.*, 2007, **19**, 4535–4538.
259 T. Kawamoto, K. Kurata, T. Mori and R. Kumai, *J. Phys. Soc. Jpn.*, 2021, **90**, 103703.
260 T. Kadoya, S. Sugiura, T. Higashino, K. Tahara, K. Kubo, T. Sasaki, K. Takimiya and J. Yamada, *Crystals*, 2021, **11**, 868.
261 T. Kadoya, M. Shishido, S. Sugiura, T. Higashino, K. Tahara, K. Kubo, T. Sasaki and J. Yamada, *Chem. Lett.*, 2022, **51**, 683–686.

